Strain Transfer between a CPC Coated Strain Gauge and Cortical Bone during Bending

Nicholas M. Cordaro,[1] Jeffrey A. Weiss,[1,2] John A. Szivek[1,3]

[1] Biomedical Engineering Program, The University of Arizona, 1300 N. Mountain, Rm. N509, Tucson, Arizona 85721

[2] Department of Bioengineering, The University of Utah, 50 S. Central Campus Dr., #2480, Salt Lake City, Utah 84112

[3] Department of Orthopedic Surgery, The University of Arizona, 1501 N. Campbell, P.O. Box 245064, Tucson, Arizona 85724–5064

Received 30 May 2000; revised 10 October 2000; accepted 13 October 2000

Abstract: The finite element method was used to simulate strain transfer from bone to a calcium phosphate ceramic (CPC) coated strain gauge. The model was constructed using gross morphometric and histological measurements obtained from previous experimental studies. Material properties were assigned based on experiments and information from the literature. Boundary conditions simulated experimental cantilever loading of rat femora. The model was validated using analytical solutions based on the theory of elasticity as well as direct comparison to experimental data obtained in a separate study. The interface between the bone and strain gauge sensing surface consisted of layers of polysulfone, polysulfone/CPC, and CPC/bone. Parameter studies examined the effect of interface thickness and modulus, gauge geometry, partial gauge debonding, and waterproofing on the strain transfer from the bone to the gauge sensing element. Results demonstrated that interface thickness and modulus have a significant effect on strain transfer. Optimal strain transfer was achieved for an interface modulus of approximately 2 GPa. Strain transfer decreased consistently with increasing interface thickness. Debonding along the lateral edges of the gauge had little effect, while debonding proximal and distal to the sensing element decreased strain transfer. A waterproofing layer decreased strain transfer, and this effect was more pronounced as the modulus or thickness of the layer increased. Based on these simulations, specific recommendations were made to optimize strain transfer between bone and CPC coated gauges for experimental studies. © 2001 John Wiley & Sons, Inc. J Biomed Mater Res (Appl Biomater) 58: 147–155, 2001

Keywords: strain gauge; bone; strain measurement; finite element analysis

INTRODUCTION

The remodeling of bone in response to mechanical stimuli has been a topic of interest and significance in both basic and clinical orthopedic research for over a hundred years. Although the exact mechanism of mechanotransduction by bone cells still remains unknown, methods for the study of mechanical variables *in vivo* are an important part of the study of bone remodeling and mechanotransduction. The difficulties associated with the *in vivo* measurement of mechanical quantities are quite extensive. One of the most fundamental measurements that must be made is the change in strain patterns that may occur in a bone after a specific treatment or other stimulus.

The foil strain gauge has become an important tool for the study of *in vivo* bone strains. Lanyon and Smith[1] documented the use of *in vivo* strain gauges bonded to bone with isobutyl 2-cyanoacrylate on sheep tibiae to record strain. A similar procedure was used by Lanyon[2] to study strain behavior on sheep lumbar vertebrae during gait. This lead to developmental methods for researching the mechanical environment present on the bone surface. Lanyon et al.[3] studied bone strain on the proximal femur of sheep after a total hip replacement. They studied the bone strain near the implant, bone resorption, and implant loosening. Although useful for securing strain gauges for immediate measurements *in vivo*, cyanoacrylate begins to dissolve within a few hours and dissolves to the point that strain sensing becomes inaccurate within a couple of weeks when used *in vivo*. Its resorption is associ-

Correspondence to: Jeffrey A. Weiss, Ph.D., Department of Bioengineering, University of Utah, 50 S. Central Campus Drive, Rm. 2480, Salt Lake City, Utah 84112 (e-mail: jeff.weiss@utah.edu)

Contract grant sponsor: National Science Foundation; contract grant number: 9807623

Contract grant sponsor: Whitaker Foundation

Publication to be a portion of a thesis, submitted in partial fulfillment of the requirements for a master's degree at The University of Arizona.

ated with the release of potentially harmful degradation products. Acrylics, polyurethanes, and epoxy resins also exhibit poor biocompatibility and are difficult to use when bonding to a smooth bone surface.[4] Because of these difficulties, improved methods for bonding of strain gauges to bone for *in vivo* measurements have been sought.

CPCs such as resorbable tricalcium phosphates and bioactive hydroxyapatite ceramics have been used to coat orthopedic implants to induce bone bonding.[5] Calcium phosphate ceramic (CPC) particles can be used to bond strain gauges to bone. The CPC particles induce bone growth and attachment, permitting strain transfer from the bone surface to the strain gauge. This technique has been used to bond gauges to cortical bone in both the rat[6] and dog models,[7,8] and has allowed accurate strain measurements for up to 18 weeks in the canine model.[9]

Strain transfer between the bone and CPC coated strain gauges is not fully understood. Combined biomechanical and histological studies have illustrated that an accurate strain reading may be achieved even with partial bonding or irregular in-growth of bone around the CPC particles.[8,10] The effect of bone growth over the edges of the gauge will also likely affect the measured strain. Factors such as waterproofing materials or the thickness of CPC and polysulfone layers may be important parameters to consider when designing gauge attachment protocols for *in vivo* experiments. These variables are difficult to examine experimentally because of the small size of sensors and the large number of experimental parameters.

The objective of this study was to create and validate a finite element model of strain transfer between cortical bone and a strain gauge. The finite element model was subsequently used to perform parameter studies on the effects of interface modulus, interface thickness, gauge geometry, waterproof coating, and partial gauge debonding. It was hypothesized that a thicker layer between bone and gauge would reduce strains, as would an interface that was too hard or too soft. It was also hypothesized that waterproofing layer thickness would affect the effective strain sensed by the strain gauge.

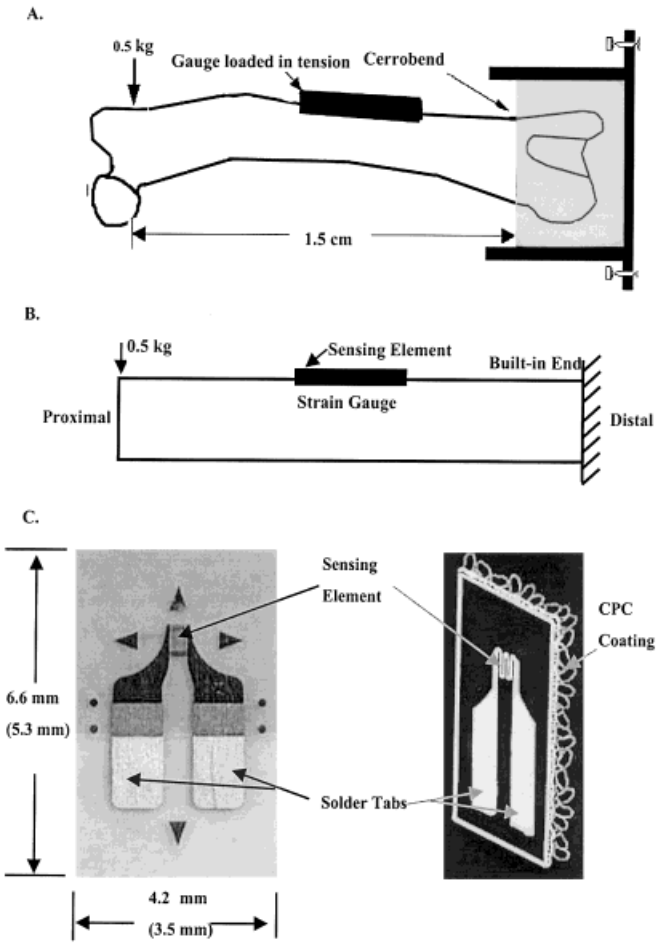

Figure 1. (A) Experimental configuration for bending tests on rat femora. (B) Geometry and boundary conditions used in the finite element studies. (C) Detail of strain gauge and sensing element.

MATERIALS AND METHODS

Experimental System

The finite element model was constructed to mimic an *in vivo* experimental system that was used to monitor strains in rat femora.[11] A brief description of the experimental methodology and results is presented here to provide the reader with a framework to better understand the choices for finite element model geometry, material properties, and interpretation of the model validation by comparison to experimental strain data. In this separately published experimental study, a number of different surface enhancements including TGF-β and Osteogenic Protein-1 were compared to the unenhanced CPC coated surface using groups of six Sprague–Dawley rats as the animal model. The data for the unenhanced group were used for validation of the finite element models in the present study. Strain gauges (CEA-06-15UW-120, Measurements Group, Raleigh, NC) were coated with a CPC blend (15 wt% CPC 6 and 85 wt% CPC 7, Biointerfaces Inc., San Diego, CA) to accelerate gauge bonding to rat femora. The sensing surface of each gauge was coated with a thin layer of medical grade 15 wt% polysulfone (PS) (Amoco, Huntington Beach, CA) to attach the CPC particles to the gauge surface. The gauges were sterilized and then each gauge was placed on the lateral aspect of a rat's femur, during aseptic surgery, using circumferentially placed resorbable sutures to temporarily secure the gauges on the cortex. After three weeks, animals were sacrificed and the femora were harvested for mechanical testing. An uncoated strain gauge was glued using cyanoacrylate to the contralateral femur in the same location as the implanted gauge. The bones were embedded in a low melting point allow and tested in cantilever bending using a published procedure[6] [Fig. 1(A)–(B)]. Loading was applied via a servohydraulic test machine (Materials Testing Systems Corporation, Minneapolis, MN) at a rate of 4.905 N/s to a load of 4.905 N (0.5 kg). A percent sensing accuracy for the CPC

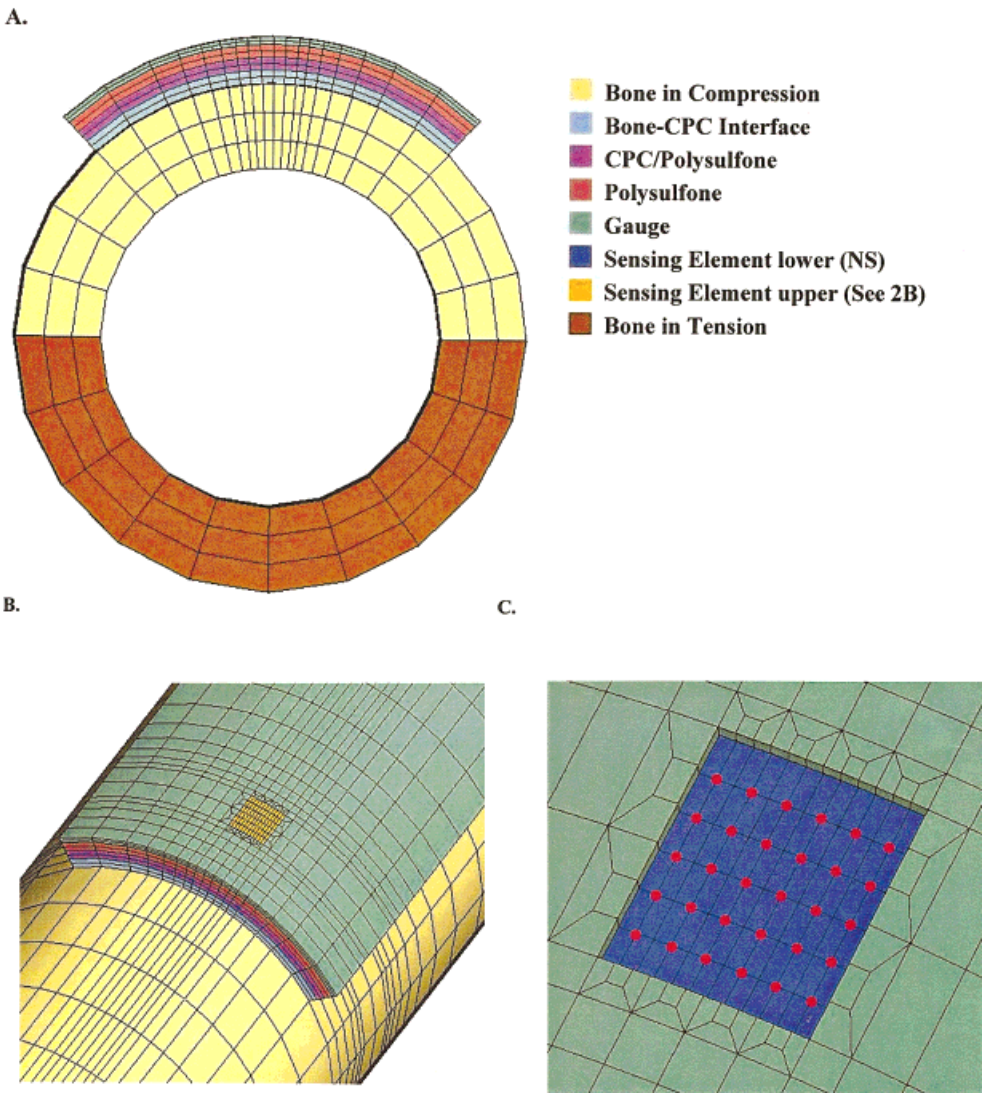

Figure 2. Finite element mesh used for parameter studies. (A) Axial view, illustrating the discretization and the layers between the bone and strain gauge. (B) Close-up view of the strain gauge. (C) Close-up view of element discretization of the gauge sensing region. Nodes used to determine sensing element average strain are show in red.

coated strain gauge was calculated and used to compare the mechanical behavior of the CPC coated strain gauges between the glued controls and different test groups. Using this methodology, the ability of the CPC coated strain gauges to sense strain could be directly compared to a contralateral bone with the glued gauge.

Finite Element Model Geometry

The finite element mesh was constructed using a commercial preprocessing package (TrueGrid, XYZ Scientific, Livermore, CA). The mesh was parameterized to allow changes in overall geometry without altering mesh topology or element count. The rat femur was represented as a thick-walled cylinder with an inner diameter of 2.6 mm, outer diameter of 3.9 mm, and length of 25.0 mm [Fig. 2(A)–(B)]. These dimensions represented average values of gross and histomorphometric measurements obtained from the experimental study.[11] The long axis of the cylinder was aligned with the global *z*-axis, while the tangent of the strain gauge normal vector was placed in the *x*-*y* plane. The thickness of the strain gauge (0.056 mm) was taken from literature supplied by the manufacturer [Fig. 1(C)], while the outer dimensions (6.60 $\times$ 4.20 mm), sensing element dimensions (0.50 $\times$ 0.35 mm) and position of the sensing element were taken from measurements made with digital calipers. The strain gauge was assumed to lie uniformly on the bone. The strain gauge is constructed of a top and bottom layer of polyimide, with the foil sensing wire sandwiched between the polyimide layers. The two polyimide layers of the gauge were modeled separately so that strain readings could be obtained at the same radial position as the sensing wire. A highly refined mesh was created to represent the sensing element [Fig. 2(C)], so that

the strains experienced by the lengths of the compliant foil sensing wire could be integrated to yield an average sensing element strain. Detailed transition regions were incorporated into the finite element mesh to integrate this refined portion of the mesh with the rest of the model.

Dimensions and regions of the interface between the bone and strain gauge were chosen to yield a finite element model geometry that would represent the bone-gauge composite after bony integration of the strain gauge. Histological analyses of the *in vivo* model provided the information regarding the total interface thickness and the constituent layers of the interface. Based on histological measurements, the total interface thickness between the bone and the CPC coated strain gauge was approximately 0.3 mm.[11] On histological sections, three distinct regions were noted between the cortical bone surface and the gauge: a layer composed primarily of CPC particles and newly formed bone, a layer of CPC and polysulfone, and a layer of polysulfone. For the finite element analyses that incorporated all three layers, these layers were assumed to have equal thickness [Fig. 2(A)].

Material Properties

All materials were represented with an isotropic hypoelastic constitutive model in the finite element code. Hypoelasticity is a generalization of linearized elasticity to large strains and rotations.[12] Material properties were separately assigned to each material region indicated in Figure 2(A). The bone was assumed to be isotropic and homogeneous, and the elastic moduli of the bone were based on experimental studies of 120-day-old Sprague–Dawley rat femora.[13] The bone moduli were 22.36 and 20.5 GPa for compression and tension, respectively. An elastic modulus of 2.8 GPa was used for the strain gauge material (type 6/6 polyamide).[14]

The material properties of the interface matrix were unknown. The modulus for pure hydroxyapatite is between 41.5 and 180.5 GPa,[15] while the modulus of pure polysulfone is 2.5 GPa.[16] However, the composite modulus depends on the distribution and relative volume fraction of the CPC particles in the polysulfone, bonding between the two materials, the in-growth of new bone around the CPC particles near the cortical shell. The CPC/polysulfone composite cannot be easily subjected to material testing, because it is both brittle and thin. Thus, the moduli of the interface layers were introduced as parameters in the finite element studies, as detailed in the sections below.

The elastic modulus of the polysulfone was determined from a tensile test performed in this study. A thin sheet of polysulfone was created using a standard protocol for gauge preparation.[10] A dumbbell-shaped sample was punched from the polysulfone sheet. The sample was gripped using custom clamps and loaded in tension at 0.25 mm/s until failure occurred. From measurements of stress and strain, the elastic modulus was determined to be 1.89 GPa, which was slightly lower than a reference value of 2.5 GPa.[16] The value determined from this experiment was used for polysulfone in all finite element studies. Poisson's ratio for all interface materials was set to 0.3. A parameter study of this material property was conducted during the early phases of the study. Variations of this parameter caused negligible changes in the average axial strain recorded at the sensing element.

Boundary Conditions and Solution Method

Because the end of the bone is typically potted in a low-melting alloy for mechanical testing in bending, the $z = 0$ end of the cylinder was modeled as built-in by prescribing fixed boundary conditions [Fig. 1(C)]. A load of 4.905 N was applied to the cylinder at the opposite end in the same plane as the sensing element, placing the strain gauge in tension. Finite element analyses were performed using the three-dimensional, nonlinear, implicit finite element code NIKE3D.[17] Trilinear hexahedral brick elements were used to represent all materials in the model. A quasi-static analysis was performed, with the load applied in increments. Because of the large deflections and rotations experienced by the bone-gauge composite during loading, a nonlinear, incremental-iterative solution strategy was used with a quasi-Newton procedure governing the iterative process.[18] Convergence at each increment in applied load was based on the norm of the change in incremental nodal displacements.

A convergence study was performed to ensure that the mesh was sufficiently refined in areas of large stress gradients. The final mesh consisted of a total of 7,538 elements and 10,332 nodes, with 6 elements through the thickness of the interface separating the bone from the strain gauge [Fig. 2(A)–(B)]. A mesh of 9 elements through the thickness yielded the same average sensing element z-strain as 6 elements. Mesh geometry was further refined by optimizing element aspect ratios and maximizing orthogonality of element edges.

Data Reduction and Analysis

For each finite element analysis, the average axial strain value at the sensing element was found by averaging the nodal axial strains within the center of the sensing element [Fig. 2(C)]. The nodal locations were evenly spaced along the approximate locations of the sensing element wires. Because the bone and gauge underwent large deflections and rotations (but small strains) during loading, the Green–Lagrange strain components were used for strain comparisons. The Green–Lagrange strain components are equivalent to those of the infinitesimal strain tensor when the strains are small enough to justify application of the linearized theory of elasticity and are unaffected by rigid body rotations, unlike the infinitesimal strain tensor components.[19]

Model Validation

Validation of initial finite element model was achieved in several steps. First, the strains predicted by the bone model without any gauge or interface material were compared to the analytical solution of a built-in cantilevered beam with tip loading based on the theory of elasticity. Second, strains

predicted for a perfectly bonded strain gauge were compared to those of the model without a gauge. Finally, the strains obtained for the bones tested in cantilever bending with strain gauges glued to the surface of the bone in the experiments of Cordaro et al.[11] were compared to the results of finite element simulations of a gauge bonded directly to the bone. To determine the optimal experimental configuration needed to maximize strain transfer from the bone surface to the strain gauge sensing element and assess the variability that would be induced by a number of experimental factors, a series of parameter studies were carried out as detailed in the paragraphs that follow.

Effect of Interface Properties and Thickness

To examine the model sensitivity to overall interface properties, the predicted axial strain was determined for interface elastic moduli of 0.15, 1.0, 1.5, 1.89, 2.0, 10, 15, 20, and 50 GPa. This was conducted to develop an understanding of the general behavior of the model with variations in the bone–gauge interface. To simulate the effect of partial to full bone/CPC attachment, a parameter study of the bone to CPC interface was conducted using the same moduli. To study the effects of bone to CPC attachment and associated CPC/PS ratio, parameter studies of these interface layers were conducted as well. For the latter three parameter studies, the rest of the interface was left at 1.89 GPa (modulus of polysulfone). Finally, the total interface thickness was varied from 0.15–0.45 mm with (E = 1.89 GPa) to study differences in CPC coating thickness variations observed during the experimental study.

Effect of Gauge Debonding, Waterproofing, and Trimming

Histological sections of the gauge-bone complex sometimes show regions of nonbonding between the gauge and bone. These regions are typically along the sides or at the ends of the gauge. The effect of gauge debonding was assessed by removing the CPC–bone interface on the lateral sides and posterior and anterior sides of the strain gauge independently. The effect of a waterproof coating was studied by adding a 0.3 mm thick layer over the top of the gauge and varying its elastic modulus between 1, 2, 4, and 10 GPa. In some of our experimental studies, the gauges were trimmed to provide a better fit onto the bone. To understand the potential effects of this modification, approximately 1 mm was removed from each side and then the strain gauge was trimmed to a length of 5.3 mm.

RESULTS

Finite element solutions were obtained without difficulty using four increments in applied bending load. Axial strains along the tensile surface of the bone varied linearly along the length, with zero axial strain at the built-in end and maximum axial strain at the loaded end, as expected based on linear elastic beam theory [Fig. 3(A)]. The lower section of the bone was in compression while the top was in tension.

Model Validation

Without a gauge present, predicted tip deflection from the finite element model at the point of applied load and axial strain at the center of the sensing element were 0.14 mm and 512 $\mu\epsilon$, respectively. Simple beam theory predicted values of 0.13 mm and 514 $\mu\epsilon$, indicating excellent agreement between the finite element analysis and the predictions based on elasticity theory. Strain transfer from the bone to the glued gauge was nearly complete [Fig. 3(A)–(B)]. However, there was a subtle difference in the strain contours even for this case. The average axial strain at the location of the sensing element was 539 $\mu\epsilon$ for the glued gauge, compared to 512 $\mu\epsilon$ for the bone in the same location. The higher strain with the perfectly bonded strain gauge is to be expected, because the gauge surface is farther from the neutral axis of the system than the case without the gauge. The finite element prediction for the average sensing element strain for the glued gauge (539 $\mu\epsilon$) were lower than those obtained from the experiments in Cordaro et al.[11] (612 $\pm$ 101 $\mu\epsilon$), but were within a single standard deviation of the mean.

Effect of Interface Properties and Thickness

The parameter studies of the interface elastic moduli for simulation of a CPC coated strain gauge showed that maximum strain transfer occurs between the bone and gauge for the situation when the elastic modulus of the entire interface was approximately 2 GPa (Fig. 4). The sensing element axial strain rapidly declined when modulus dropped below 1 GPa, and gradually declined for values above 2 GPa. This effect was more pronounced with the variations of the CPC–bone interface than with the CPC–PS interface. As the total interface thickness was varied, a thickness of greater than 0.15 mm began to reduce the sensing element axial strains [Fig. 5(A)].

Effect of Gauge Debonding, Waterproofing, and Trimming

Reduction of the elastic modulus of the lateral sides of the CPC–bone interface induced negligible changes in the average axial strain on the sensing element (504 vs. 505 $\mu\epsilon$). When the interface along the sides was removed entirely, the sensing strain increased to 516 $\mu\epsilon$ (Fig. 6). However, by softening and then removing the proximal and distal ends of the interface, the strain reduced to 487 and 380 $\mu\epsilon$, respectively. These results highlight the importance of adequate axial bonding in comparison to bonding of the lateral sides.

A waterproofing layer with a modulus of 1 GPa reduced the sensing element recorded axial strain to 444 $\mu\epsilon$, a 12% reduction [Fig. 5(B)]. When the modulus was increased to 2 GPa, the strain was further reduced to 402 $\mu\epsilon$, or a 21% reduction. A waterproof coating with an elastic modulus of 4

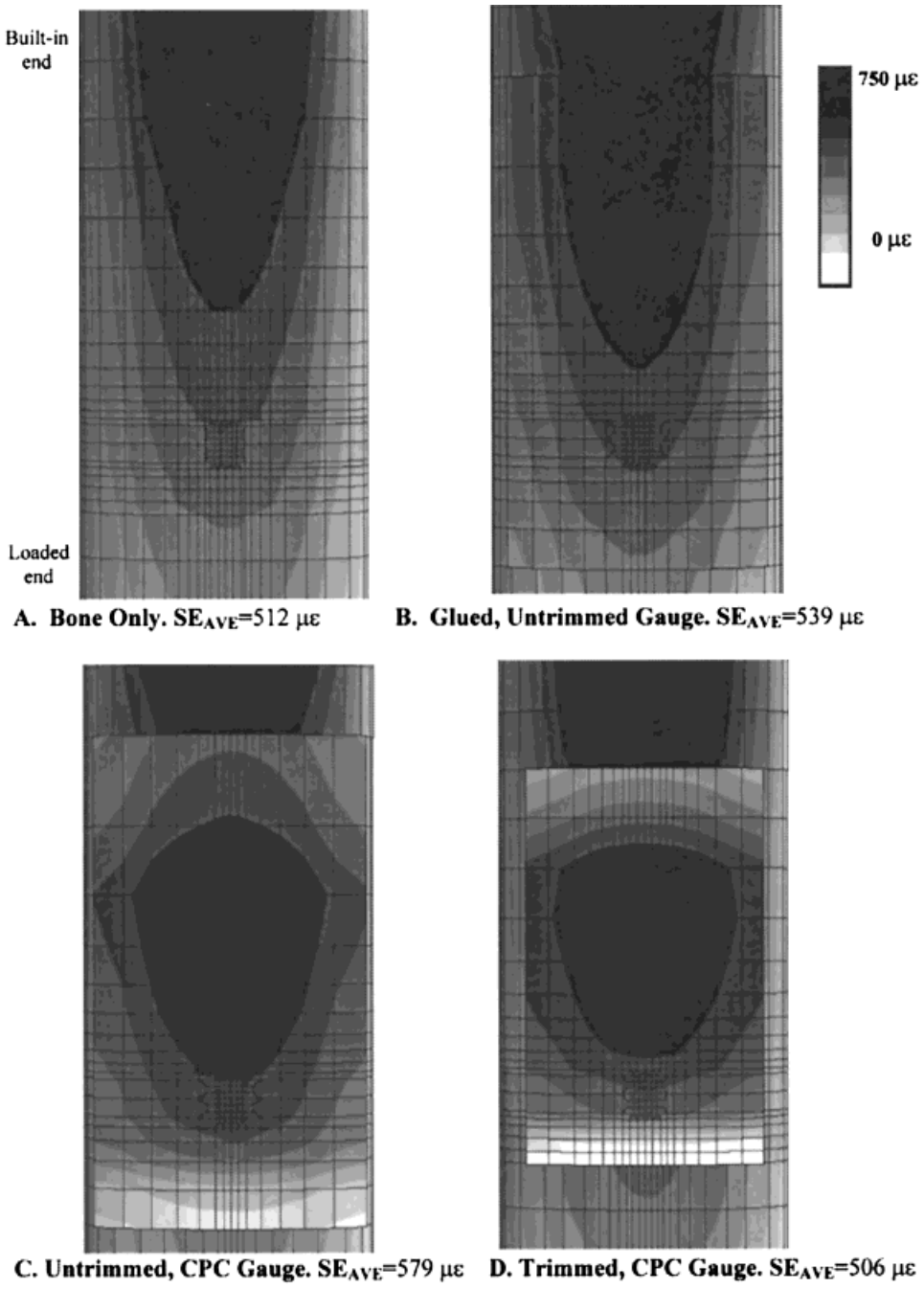

Figure 3. Contour/fringe plots of axial strain. (A) Bone without a strain gauge. (B) Glued (perfectly bonded) strain gauge. (C) Untrimmed gauge geometry. (D) Trimmed gauge geometry used in the experimental model. The modulus of the entire interface was 1.89 GPa for the latter two analyses.

and 10 GPa further reduced the sensing element *z*-strain by 32% and 49%, respectively.

The effective strain transfer from the bone to the untrimmed strain gauge versus the trimmed gauge was 13% different [Fig. 3(C)–(D)]. An area of high axial strain was present in the central regions of both gauges and the proximal side of the gauge (closest to the sensing element) was at a zero strain. By trimming the strain gauge, the sensing element was moved into this region of lower strain, reducing the average sensing element *z*-strain from 583 to 510 $\mu\epsilon$. Figures 3(C)–(D) also show the large axial gradients in strain across the strain gauge and sensing element, highlighting the importance of consistent placement of the gauges along the long axis of the bone for experimental studies utilizing a cantilever beam test configuration.

DISCUSSION

This study analyzed strain transfer between cortical bone and an attached strain gauge. The geometry and material proper-

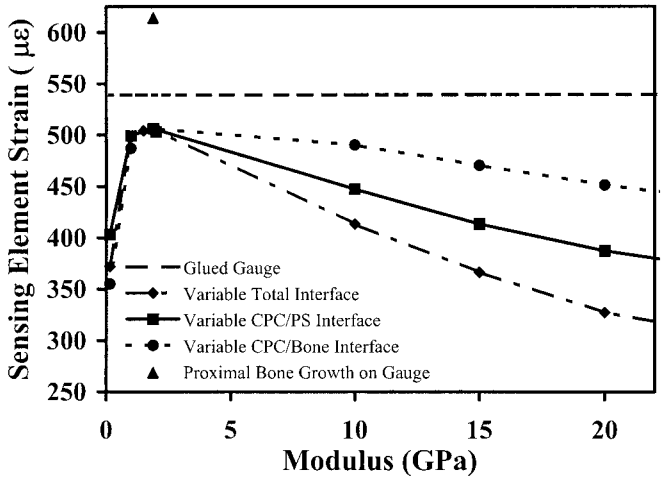

Figure 4. Parameter study of the interface between the gauge and bone. Unless specified, modulus for other interface layers is $E = 1.89$ GPa. Results for interface values between 1–2 GPa were closest to the glued gauge axial strain values. Changes in the total interface modulus had the largest effect on the measured strain, followed by changes in the CPC-PS interface, and finally the CPC–bone interface. As interface modulus was decreased, sensing strain dropped off rapidly.

ties used in the model represented both published and experimentally determined values. The finite element model was validated by a series of convergence studies, model refinements, and comparison to both theoretical predictions and experimental measurements. Excellent agreement was obtained between the finite element predictions and the elasticity solution for strain on the surface of the bone without a gauge present. Finite element strain predictions for the case of a glued gauge were in reasonable agreement with strain values recorded experimentally for the case of a gauge glued directly to the bone. Differences between the finite element predictions and the experimental strain values were within a single standard deviation of the experimental data, and can likely be attributed to inhomogeneities in material properties and geometry that were not included in the finite element model definition. Specifically, the finite element model assumes perfectly cylindrical bone geometry and uniform modulus and Poisson's ratio. The differences do not affect the validity of the conclusions obtained from the parameter studies of sensitivity of the strain field to changes in interface elastic modulus, gauge and interface dimensions, debonding, and the waterproof coating. All these parameters had large effects on the strain transfer from the bone surface to the gauge sensing element.

The parameter studies of the bone–gauge interface elastic moduli demonstrated the effect of alterations of the interface modulus. Both the PS layer and the CPC/PS layer can be controlled experimentally. However, as the bone grows into the CPC coated strain gauges, the effective elastic modulus changes. When the total interface thickness was increased above 0.15 mm, the computed sensing element axial strain was decreased. The large CPC particles used in the experimental studies of Cordaro et al.[11] were 561 ± 112 μm by 115 ± 70 μm. These were blended with smaller particles, which were 9 ±7 μm by 6 ± 5 μm. With the large particles oriented with their long axis parallel to the gauge surface and with a typical 0.1 mm thickness of polysulfone, the interface thickness is approximately 0.22 mm. Histology showed the large particles oriented with their long axis in a variety of directions, and they were often 2 or 3 CPC particle layers thick. Analytically, a 0.45 mm interface thickness reduces the sensing element axial strain by as much as 17% in comparison to the case of a glued gauge. It is possible that this effect offsets the effect of bone growth along the proximal edge of the strain gauge in the experimental model.

Immediately after gauge implantation, there is no bonding between the bone and CPC particles. Fibroblasts, macrophages, and giant cells cover the area between the gauge and the bone. Eventually, osteoblasts lay down a collagen matrix, attaching the bone to the CPC particles. This layer has a low effective elastic modulus. This layer begins to calcify into areas of woven bone infiltrated with cells such as other

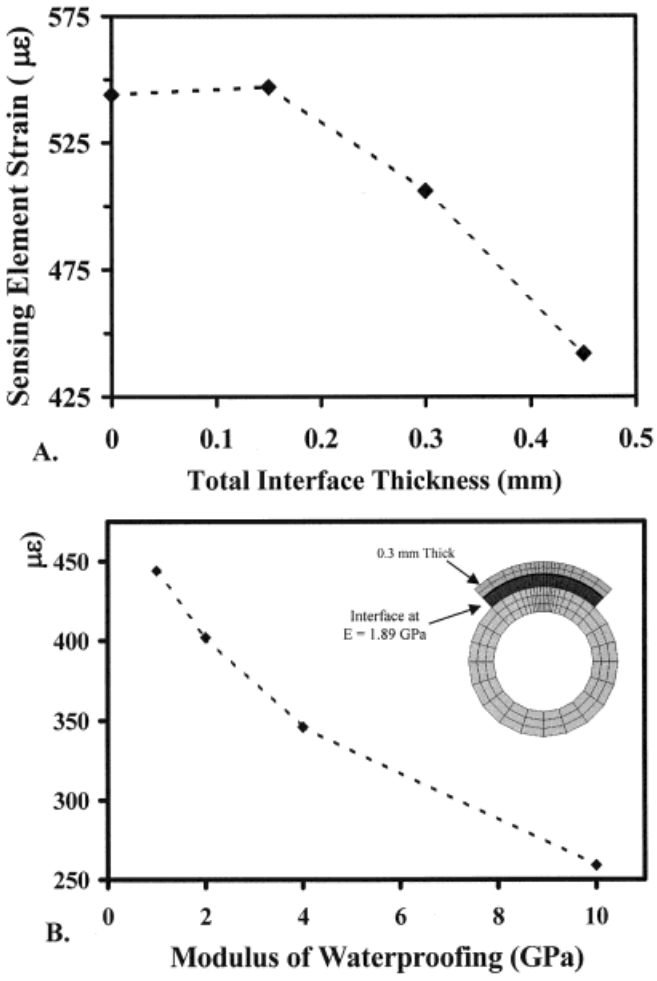

Figure 5. (A) Effect of interface thickness on sensing element strain. There was a moderate decrease in sensing element strain with increasing interface thickness. (B) Effect of waterproof coating modulus on sensing element strain. The coating thickness was held constant at 0.3 mm. Even with a modulus of 1 GPa, the measured strain was only 444 $\mu\epsilon$, still 50 $\mu\epsilon$ below the best results illustrated in Figure 5.

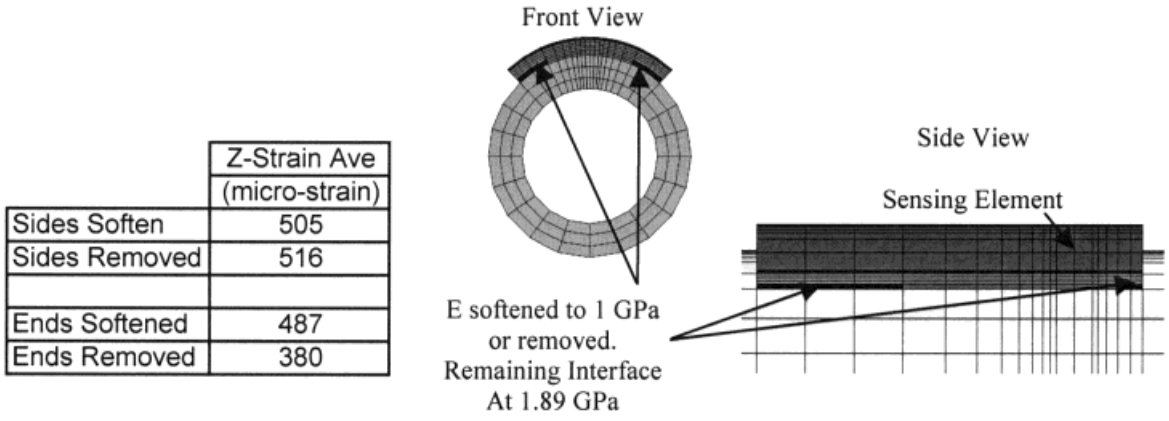

	Z-Strain Ave (micro-strain)
Sides Soften	505
Sides Removed	516
Ends Softened	487
Ends Removed	380

Figure 6. Effect of softening and debonding the CPC–bone interface on the lateral edges and the proximal and distal ends.

fibroblasts, osteoblasts, and endothelial cells forming capillaries. Woven bone, bonding the CPC particles to the preexisting cortical bone, was noted to produce a more accurate measured strain compared to a glued gauge.

Comparisons of the untrimmed and trimmed gauges demonstrated the importance of a constant gauge geometry between animals for accurate experiment comparisons. The large strain gradients along the length of the strain gauge highlight the importance of proper gauge orientation and gauge placement to accurately measure *in vivo* bone surface strain.

In the *in vivo* experiments, bone growth on the proximal and distal ends of the gauge was often noted. By improving the bonding between these ends of the gauge and the bone, strain transfer is enhanced (Fig. 3). A 0.3 mm wide section of bone extending just to the bottom surface of the strain gauge increased the sensing element axial strain by 21%. This surpassed the value measured from the glued gauge.

Debonding or softening of the lateral edges of the gauge had little effect on the predicted axial strain, while debonding or softening the front and back edges of the strain gauge reduced the axial strain in the sensing element. This demonstrates that CPC bonding in-line with the sensing element is more important for measuring axial strain. It also suggests that there must be sufficient bonding both in front of and behind the gauge sensing element to ensure proper strain transfer. To achieve bonding *in vivo*, the CPC coated strain gauge must be held securely against the bone surface while bone attachment occurs. In our experiments, resorbable sutures tied around the femur were used to achieve this. If the lateral edges of the strain gauge do not require bone to CPC bonding for long term *in vivo* strain measurements, it may be possible to glue the lateral edges of the strain gauge with an adhesive to affix the strain gauge to the bone long enough for the bone attachment to the CPC particles to occur. A gel form of cyanoacrylate would be needed to keep the glue from being wicked into the porous CPC surface.

A stiff waterproofing layer was shown to be a potential source of strain sensing error. In our *in vivo* studies, a nitrile rubber, acrylic, and polyurethane coating has been used, and these materials have a much lower modulus than epoxy. Further, we removed the materials before the experimental beam bending analysis. An epoxy coating is attractive as a potential waterproofing layer. Based on the results of this study, an epoxy layer should be as thin as possible, or a softer material should be sought for the purpose of waterproofing.

The predicted strain gauge responses used in this finite element analysis are valid only for the specific material and geometric assumptions incorporated into the model. Homogeneous material properties were assumed for all material regions indicated in Figure 2(A). This assumption is likely appropriate for the bone and strain gauge materials. However, the local distribution of new bone, CPC particles, and polysulfone in the interface layers are probably inhomogeneous. The effects of this type of distribution can be incorporated in the finite element analysis by using micromechanical modeling techniques or homogenization theory. This was beyond the scope of this study. In addition, it is likely that such model refinements would not be warranted in terms of the change in the results. A more realistic geometry could readily be incorporated into the model by using micro-CT or histological sections to yield accurate representations for the bone internal and external surfaces. Again, these changes would provide more accurate strain predictions, but would not alter the general trends demonstrated by the parameter studies.

Based on the results of this work, a number of recommendations can be made for the use of CPC coated strain gauges in experimental studies. The thickness of the interface layer should be minimized, particularly when these gauges are used in an animal model with a small bone section. This can be achieved by altering the size of the CPC particles and the thickness of the polysulfone layer used to bind the particles to the gauge. Adequate gauge material should be present both proximal and distal to the sensing element. For long-axis bending studies, the sides of the gauge can be trimmed with little effect on the measured axial strain. Due to the variations in axial strain along the long axis of the bone during the cantilever bending experiments, an alternative test configuration such as four-point bending may provide a system that is less sensitive to gauge placement along the bone long axis.

Support by the National Science Foundation grant number 9807623 and the Whitaker Foundation is gratefully acknowledged.

REFERENCES

1. Lanyon LE, Smith RN. Bone strain in the tibia during normal quadrapedal locomotion. Acta Orthop Scand 1970;41:238–248.
2. Lanyon LE. Strain in sheep lumbar vertebrae recorded during life. Acta Orthop Scand 1971;42:102–112.
3. Lanyon LE, Paul IL, Rubin CT, Thrasher EL, DeLaura R, Rose RM, Radin EL. In vivo strain measurements from bone and prosthesis following total hip replacement. J Bone Joint Surg 1981;63:989–1001.
4. Donkerwolcke M, Burny F, Muster D. Tissue and bone adhesives—historical aspects. Biomater 1998;19:1461–1466.
5. Hench LL. Bioceramics. J Am Ceram Soc 1998;81:1705–1728.
6. Szivek JA, Anderson PL, Wilson DL, DeYoung DW. Technical note: Development of a model for study of in vivo bone strains in normal and microgravity environments. J Appl Biomater 1995;6:203–208.
7. Szivek JA, Gealer RL, Magee FP, Emmanual J. Development of an HA backed strain gauge. J Appl Biomater 1990;1:241–248.
8. Maliniak MM, Szivek JA, DeYoung D. The development of hydroxyapatite coated strain gauges for long-term in vivo bone loading response measurements. J Appl Biomater 1993;4:143–152.
9. Szivek JA, DeYoung DW. In vivo strain measurements collected using calcium phosphate ceramic-bonded strain gauges. J Invest Surg 1997;10:263–273.
10. Szivek JA, Anderson PL, Dishongh TJ, DeYoung DW. Evaluation of factors affecting bonding rate of calcium phosphate ceramic coatings for in vivo strain gauge attachment. J Biomed Mater Res 1996;33:121–132.
11. Cordaro NM, Szivek JA, DeYoung DW. Surface enhancements can accelerate bone bonding to CPC coated strain gauges. J Biomed Mater Res, to appear.
12. Truesdell C, Noll W. The nonlinear field theories of mechanics. New York: Springer–Verlag; 1992.
13. Battraw GA, Miera V, Anderson PL, Szivek JA. Bilateral symmetry of biomechanical properties in rat femora. J Biomed Mater Res 1996;32:285–288.
14. Park JB. Biomaterials science and engineering. New York: Plenum; 1987.
15. Yoshimura M, Suda H. Hydrothermal processing of hydroxyapatite: past, present, and future. In: Brown PW, Constantz, editors. Hydroxyapatite and related materials. Boca Raton, FL: CPC; 1994. p 46.
16. Moach. Design engineering. Data handbook F47178. 4th revision, Section 2. 1979. p 2.
17. Maker BN, Ferencz RM, Hallquist JO. NIKE3D: A nonlinear, implicit, three-dimensional finite element code for solid and structural mechanics. In: Technical Report UCRL-MA-105268. Lawrence Livermore National Laboratory; 1990.
18. Matthies H, Strang G. The solution of nonlinear finite element equations. Int J Numer Methods Eng 1979;14:1613–1626.
19. Spencer AJM. Continuum mechanics. Essex: Longman Scientific Technical; 1980.